*Syst. Biol.* 63(4):610–627, 2014

DOI:10.1093/sysbio/syu025
Advance Access publication March 28, 2014

# Analysis and Visualization of Complex Macroevolutionary Dynamics: An Example from Australian Scincid Lizards

DANIEL L. RABOSKY[1,2,*], STEPHEN C. DONNELLAN[3,4], MICHAEL GRUNDLER[1], AND IRBY J. LOVETTE[5]

[1]*Museum of Zoology, University of Michigan, Ann Arbor, MI* 48109, *USA;* [2]*Department of Ecology and Evolutionary Biology, University of Michigan, Ann Arbor, MI 48109, USA;* [3]*South Australian Museum, North Terrace, Adelaide 5000, Australia;* [4]*Australian Centre for Evolutionary Biology and Biodiversity, University of Adelaide, Adelaide 5005, Australia;* [5]*Cornell Lab of Ornithology, Cornell University, Ithaca, New York 14850, USA;* [*]*Correspondence to be sent to: Museum of Zoology, University of Michigan, Ann Arbor, MI 48109, USA; E-mail: drabosky@umich.edu.*

*Received 6 November 2013; reviews returned 19 January 2014; accepted 19 March 2014*
*Associate Editor: Vincent Savolainen*

*Abstract*.—The correlation between species diversification and morphological evolution has long been of interest in evolutionary biology. We investigated the relationship between these processes during the radiation of 250+ scincid lizards that constitute Australia's most species-rich clade of terrestrial vertebrates. We generated a time-calibrated phylogenetic tree for the group that was more than 85% complete at the species level and collected multivariate morphometric data for 183 species. We reconstructed the dynamics of species diversification and trait evolution using a Bayesian statistical framework (BAMM) that simultaneously accounts for variation in evolutionary rates through time and among lineages. We extended the BAMM model to accommodate time-dependent phenotypic evolution, and we describe several new methods for summarizing and visualizing macroevolutionary rate heterogeneity on phylogenetic trees. Two major clades (*Lerista*, *Ctenotus*; >90 spp. each) are associated with high rates of species diversification relative to the background rate across Australian sphenomorphine skinks. The *Lerista* clade is characterized by relatively high lability of body form and has undergone repeated instances of limb reduction, but *Ctenotus* is characterized by an extreme deceleration in the rate of body shape evolution. We estimate that rates of phenotypic evolution decreased by more than an order of magnitude in the common ancestor of the *Ctenotus* clade. These results provide evidence for a modal shift in phenotypic evolutionary dynamics and demonstrate that major axes of morphological variation can be decoupled from species diversification. More generally, the Bayesian framework described here can be used to identify and characterize complex mixtures of dynamic processes on phylogenetic trees. [Bayesian; diversification; evolvability; lizard; macroevolution, punctuated equilibrium, speciation.]

A number of evolutionary models have proposed that species diversification should be positively correlated with phenotypic evolution (Eldredge and Gould 1972; Pennell et al. 2013). For example, ecological and reproductive character displacement can lead to an association between speciation and phenotypic change (Schluter 2000; Pfennig D.W. and Pfennig K.S. 2013). Indeed, any model whereby speciation is associated with ecological divergence (Schluter 2000; Price 2008; Nosil 2012) can potentially lead to a positive association between speciation and morphological evolution. A common theme underlying many of these models is that they propose a role for extrinsic ecological opportunity as a driver of species diversification (Glor 2010; Yoder et al. 2010). Another class of models proposes that the capacity of lineages to evolve novel phenotypes can promote species diversification, through several different mechanisms (Vermeij 1973; Liem and Osse 1975; Adamowicz et al. 2008; Pigliucci 2008). The key feature of these models is that evolutionary lability, evolvability, or innovation is itself an intrinsic property of individual lineages (Lovette et al. 2002) that facilitates speciation (Rabosky 2012; Rabosky and Adams 2012). Even Darwin's original model for the origin of species proposed a central role for character divergence during the speciation process (Darwin 1859; Reznick and Ricklefs 2009; Pfennig D.W. and Pfennig K.S. 2013; Rabosky 2013). Darwin held that competitive interactions between closely related species were so severe that extinction was almost inevitable in the absence of ecological character divergence.

Regardless of the underlying causal mechanisms, a growing body of empirical research suggests that species diversification and morphological evolution are frequently coupled in nature. The evidence for this relationship comes not only from the fossil record (Cheetham 1986; Hunt 2007, 2008; Raia et al. 2013) but also from studies using time-calibrated phylogenetic trees of extant organisms (Mattila and Bokma 2008; Ingram 2011). Most recently, several studies have directly tested whether rates of morphological evolution are associated with rates of species diversification. This is not necessarily the same as testing for punctuated equilibrium (Adams et al. 2009), because such rate coupling need not imply that phenotypic change occurs in direct association with speciation events (Rabosky 2012). Only a few such studies have been performed using phylogenetic data, but positive relationships have been observed between rates of speciation and morphological evolution in salamanders (Rabosky and Adams 2012) and across 7000 species of ray-finned fishes (Rabosky et al. 2013).

In this study, we explore the relationship between species diversification and rates of body size and shape evolution in a large radiation of Australian scincid lizards. We focus on the Australian sphenomorphine skinks, a clade of approximately 250 species that has diversified into a morphologically and ecologically

diverse set of taxa. Two genera within this group (*Lerista* and *Ctenotus*) account for approximately 75% of the overall species diversity and appear to have undergone an increase in their diversification rate relative to other Australian sphenomorphine lineages (Rabosky et al. 2007). The Australian sphenomorphines show remarkable variation in body form, and the group is well-known for repeated evolution of limb reduction (Greer 1989; Skinner et al. 2008; Skinner 2010). Virtually the entire set of tetrapod limb conditions, from fully pentadactyl limbs to limblessness, can be found within the clade.

We constructed a time-calibrated phylogeny for the Australian sphenomorphine radiation that is >85% complete at the species level and collected morphometric data for nearly 75% of described species. Relative to previous studies (Rabosky et al. 2007), our molecular taxon sampling more than doubles phylogenetic coverage of *Ctenotus*. To model rates of morphological evolution and species diversification across the group, we generalized a recent Bayesian method for studying trait evolution (Rabosky et al. 2013; Rabosky 2014) to allow for time-varying rates of character change.

This method and associated implementation is a novel framework for the visualization and analysis of complex macroevolutionary dynamics on phylogenetic trees. BAMM enables reconstruction of branch-specific rates of speciation, extinction, and phenotypic evolution and allows rates to vary both through time and among lineages. Using BAMM, we present novel approaches for visualizing macroevolutionary dynamics, for comparing evolutionary rates across clades, and for reconstructing the location of rate shifts on phylogenetic trees. Our results suggest that the Australian sphenomorphine skinks constitute an extreme example of heterogeneous phenotypic evolutionary dynamics within a single evolutionary radiation. In contrast to recent studies on other taxa (Mattila and Bokma 2008; Ingram 2011; Rabosky et al. 2013; Raia et al. 2013), we find strong evidence that rates of morphological evolution are decoupled from rates of species diversification.

## Materials and Methods

### *Phylogeny of Sphenomorphine Skinks*

We reconstructed a species-level phylogeny for Australian sphenomorphine skinks that included more than 85% of the currently recognized species diversity in the group. We sequenced mitochondrial and nuclear loci from 89 species of *Ctenotus* skinks; 53 of these species have not been included in previous phylogenetic studies and their inclusion here greatly expands our phylogenetic framework for this diverse vertebrate genus. We combined these data with sequences from other Australian sphenomorphine skinks that were available through Genbank and which were published as part of several previous studies on sphenomorphine skink phylogenetics (Reeder 2003; Rabosky et al. 2007, 2011; Skinner 2007; Skinner et al. 2008, 2013). Molecular genetic methods have been described previously (Rabosky et al. 2011). Sequence data included four mitochondrial genes (12S rRNA, 983 bp; 16S rRNA, 556 bp; cytochrome *B*, 1143 bp; and ND4, 759 bp) and two nuclear introns (LDLR, 600 bp; ATP synthetase beta subunit intron, 550 bp). Our final data matrix contained sequences from 239 individuals, including 216 species of the monophyletic Australian sphenomorphine clade (Reeder 2003; Rabosky et al. 2007; Skinner et al. 2011) and five additional sphenomorphine taxa from other regions. Excluding sites that contained a single nucleotide (e.g., those with alignment gaps or missing data at all but one site), our data matrix were approximately 64% complete. Although several species were represented by sequence data for a single gene, 97.8% of taxa in our matrix contained at least 2000 bp of nucleotide data and had data for three genes (ND4, 12S rRNA, and the ATP synthetase intron). Museum voucher numbers and GenBank numbers are provided in the electronic Supplementary Material (Appendix 1: Supplementary Tables S1 and S2, http://doi.org/10.5061/dryad.kd38f).

We used relaxed clock Bayesian methods as implemented in BEAST (Drummond and Rambaut 2007) to estimate a posterior distribution of time-calibrated phylogenetic trees. We analyzed a concatenated data set, partitioning data across genes and codons. We linked evolutionary models assigned to codon positions for the two mitochondrial protein coding genes (cytochrome *B* and ND4), but otherwise assigned each partition a separate GTR + G + I model of sequence evolution. This model was chosen over less-complex alternatives to avoid known problems associated with the use of underparameterized models of sequence evolution (Lemmon and Moriarty 2004). We placed lognormal prior densities on the ages of three well-supported nodes from a previous study (nodes J, K, and L from Skinner et al. 2011, table 5). Skinner et al (2011) studied the biogeography of lygosomine skinks and provided 95% credible intervals on crown ages for the Australian sphenomorphine clade, the global sphenomorphine clade, and the Papuan *Sphenomorphus* skinks. Using maximum likelihood, we estimated the parameters of the corresponding lognormal distributions that would have produced these confidence limits and incorporated them as prior densities on these three nodes in our BEAST analyses. We checked for convergence Markov Chain Monte Carlo (MCMC) runs by examining effective sizes of molecular evolutionary parameters using TRACER (Drummond and Rambaut 2007).

We did not perform explicit species tree reconstruction (Liu and Pearl 2007; Heled and Drummond 2010) for three reasons. First, our data set included high coverage for just two independent loci, and coverage for our third nuclear locus (LDLR) was relatively sparse for *Ctenotus*. Second, phylogeographic work has demonstrated that hybridization occurs between at least some species in the group (Rabosky et al. 2009). Finally, we believe that a number of species within this group are poorly defined; our ongoing work in this group suggests that

several widespread species are polyphyletic (Rabosky, unpublished data).

### *Morphometric Data*

We measured a set of external morphological characters from preserved museum specimens of 183 species in 12 genera of Australian sphenomorphine skinks. Overall, we measured 825 adult animals, for an average of 4.5 individuals per species. We measured eight characters that we expected to correlate with overall size, locomotion, and trophic ecology. These included the following: (i) snout–vent length (SVL), (ii) the maximum head height, (iii) head length, (iv) maximum head width, (v) the length of the forearm (antebrachium), (vi) femur length, (vii) length of the longest toe, and (viii) the body depth as measured at the pectoral girdle. Many previous studies have used these characters to quantify morphological variation in squamate reptiles (Harmon et al. 2003; Pinto et al. 2008; Mahler et al. 2010). Our full morphological data matrix and a detailed description of characters have been deposited in Dryad http://dx.doi.org/10.5061/dryad.kd38f. All analyses described later are based on mean trait values computed for each species.

We log-transformed all morphometric measurements prior to analysis. Among the 183 species that we measured, 31 lacked an external humerus, 6 lacked external femurs, and 7 lacked toes. We arbitrarily set all of these zero-valued measurements to 0.1 mm prior to log-transformation, although virtually identical results were obtained using a range of alternative values (0.01, 0.001). We chose to analyze the residual variation in each character after removing the correlation with a measure of overall body size (SVL). Using the maximum clade credibility (MCC) tree from phylogenetic analysis, we performed separate phylogenetic generalized least-squares (PGLS) regressions of the seven remaining morphological traits on SVL. We performed principal components analysis using the covariance matrix of phylogenetically corrected residuals. Virtually identical principal component scores were observed using phylogenetically corrected (Revell 2009) and uncorrected principal components analyses (PC1: Pearson's $r = 0.997$).

The first principal component (PC1) accounted for 84.9% of the variance in the matrix of residuals from PGLS regressions and we retained only this component for subsequent analyses. The pattern of loadings on PC1 suggests that this is an overall summary of limb reduction: forelimb, femur, and toe show loadings of −0.67, −0.45, and −0.51, respectively. Measurements associated with the head show roughly equal loadings (−0.15, −0.14, −0.15 for head depth, length, and width, respectively). Increasingly positive scores on PC1 thus reflect a reduction in limb proportions, and to a lesser degree, a decrease in relative head size, reflecting the more slender, elongate morphologies associated with fossorial or semi-fossorial limb-reduced lizards. A morphospace plot for the sphenomorphines is shown in Figure 1.

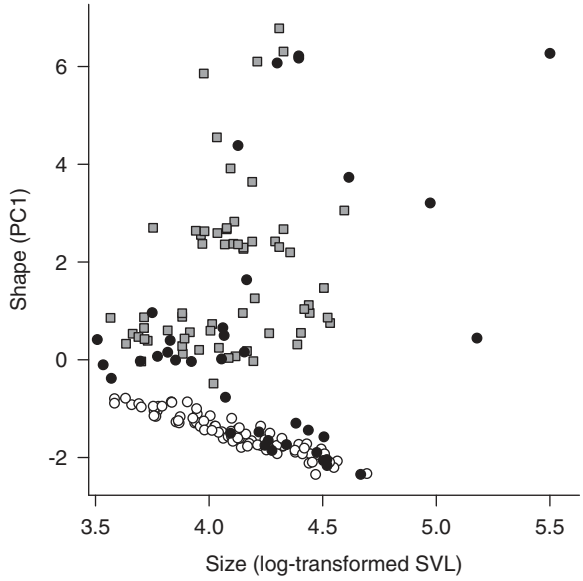


FIGURE 1. Morphospace plot for sphenomorphine skinks, including *Ctenotus* (open circles), *Lerista* (gray squares), and all other sphenomorphine species in the data set (black circles). *Ctenotus* occupies a much narrower region of shape (PC1) space than either *Lerista* or non-*Lerista*, non-*Ctenotus* sphenomorphine skinks. The distribution of body sizes (SVL) is similar across the three groups, although several species of non-*Lerista*/non-*Ctenotus* sphenomorphines are relatively large (e.g., *Coeranoscincus reticulatus; Coeranoscincus frontalis*).

### *Modeling Phenotypic Evolutionary Dynamics with BAMM*

We analyzed the tempo and mode of morphological evolution on two major phenotypic axes: body size, as reflected by SVL, and body shape, as summarized by PC1 (Fig. 1). We quantified the tempo and mode of phenotypic evolution using BAMM (www.bamm-project.org), a recently developed analysis tool for studying complex mixtures of evolutionary processes on phylogenetic trees (Rabosky 2014). The BAMM model is premised on the assumption that the distribution of morphologies in any clade reflects a complex mixture of distinct evolutionary regimes. A "regime," in this sense, is a shared dynamic process of morphological evolution or species diversification that pertains to a subset of related lineages on a phylogenetic tree (Fig. 2). Some subclades might evolve under faster (or slower) regimes of phenotypic evolution than others, but we typically do not know the location or number of distinct phenotypic regimes in advance. BAMM assumes that distinct evolutionary regimes occur across the phylogeny under a compound Poisson process (Huelsenbeck et al. 2000; Rabosky et al. 2013). Evolutionary dynamics within a single regime can involve variation in rates through time. For example, a phylogenetic tree where all lineages are governed by a single diversity-dependent slowdown in the rate of speciation or trait evolution would be

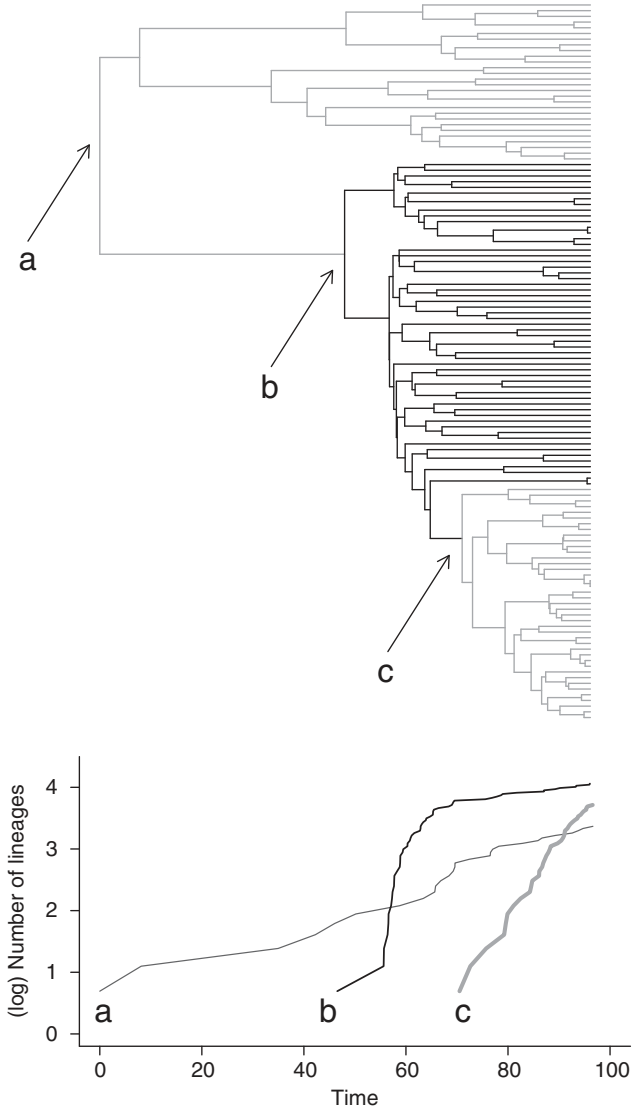


FIGURE 2. Phylogenetic tree simulated under three distinct macroevolutionary speciation regimes (top) and corresponding lineage-through-time plots for lineages belonging to each regime. (a) Constant-rate speciation regime associated with the root of the tree. (b) A single lineage shifts to a diversity-dependent speciation regime, undergoing a massive acceleration and subsequent slowdown in the rate of speciation through time. The concave-down shape of the corresponding lineage-through-time plot clearly indicates this deceleration in the rate of speciation. (c) A single lineage belonging to regime b acquires a key innovation that promotes a secondary increase in the rate of speciation. There is no requirement that regimes are associated with a particular "constant rate" process of speciation and/or extinction: a regime is simply a common rate dynamic that pertains to a portion of a phylogenetic tree and linked by common ancestry. Many real phylogenies are likely to have been shaped by a complex mixture of different regimes, but we have little a priori information about the location and nature of these regimes. BAMM uses reversible jump MCMC to identify distinct regimes of diversification and trait evolution on phylogenetic trees while making no assumptions about rate-constancy through time.

characterized by a single macroevolutionary regime. The method uses reversible jump MCMC (rjMCMC) to sample mixtures of evolutionary regimes that best explain the distribution of phenotypes across the tips of the phylogenetic tree. rjMCMC, or transdimensional MCMC, is necessary for this problem because the number of distinct regimes is estimated under the model and not fixed in advance: the Markov chain thus entails probabilistic moves between model subspaces that differ in their number of parameters. Our approach is closely related to several other rjMCMC approaches for modeling phenotypic evolution (Eastman et al. 2011; Venditti et al. 2011).

The BAMM framework builds on the general conceptual frameworks of other methods for modeling macroevolutionary rate heterogeneity, such as MEDUSA (Alfaro et al. 2009) and MOTMOT (Thomas and Freckleton 2012). However, BAMM simulates posterior distributions of rate-shift configurations and does not estimate a single "best-fit" configuration of rate shifts. The set of rate shift configurations simulated using BAMM is analogous to the credible set of tree topologies sampled using Bayesian inference software in phylogenetics. As such, BAMM affords clear advantages when multiple rate shift configurations have similar explanatory power.

BAMM provides two additional types of results that are relevant to this study. First, BAMM can provide estimates of marginal density of evolutionary rates at any point in time along any branch of a phylogenetic tree. Second, BAMM provides an estimate of the marginal density of the number of distinct evolutionary regimes, allowing immediate comparisons of sub-models with distinct numbers of evolutionary regimes. This enables researchers to ask questions such as: how much more likely is the data under a model with multiple distinct rates of trait evolution, relative to a model with a single rate?

The BAMM model was originally described for mixtures of simple Brownian motion processes across phylogenetic trees (Rabosky et al. 2013). Thus, all branches assigned to a particular evolutionary regime share a common underlying rate of phenotypic evolution at any point in time (Fig. 2). We extended the BAMM model from Rabosky et al. (2013) and Rabosky (2014) to allow phenotypic evolutionary rates to vary through time. Specifically, we assume that the occurrence of a regime shift on a branch defines a new time-inhomogeneous process of trait evolution. Thus, after the occurrence of a regime shift, the instantaneous rate (e.g., the variance of the Brownian motion process) of trait evolution, $\beta$, for all downstream lineages is governed by $\beta(t) = \beta_0 \exp(zt)$, where $\beta_0$ is the phenotypic rate at the start of the new regime, $t$ is the elapsed time from the start of the regime, and $z$ is a rate parameter that controls the magnitude of phenotypic change through time. Thus, for a phylogenetic tree with a single evolutionary regime (by definition, starting at the root node), a negative value of $z$ would imply that rates of phenotypic evolution have declined continuously through time for all lineages in the tree. Similar general models have been used to define a single diversity- or time-dependent process of trait change across a phylogenetic tree (Blomberg et al. 2003; Mahler et al. 2010; Weir and Mursleen 2013), but

our model explicitly allows for multiple independent processes and thus detects patterns of rate variation among clades. Mathematical and computational details for our implementation of the time-varying process of trait evolution are virtually identical to those described for the time-varying speciation model in Rabosky (2014).

We evaluated performance of the BAMM implementation of the time-dependent model for trait evolution by applying the method to a variety of data sets simulated under increasingly more complex scenarios of time-dependent trait change (Appendix 1, http://doi.org/10.5061/dryad.kd38f). We assessed convergence of BAMM runs by computing effective sample sizes for the likelihood of the data and for the number of distinct regimes, generally ensuring at least 200 independent post-burnin samples from the posterior. We summarized BAMM analyses by computing time-specific rates of morphological evolution, as well as clade-specific rates. To estimate clade-specific rates of phenotypic evolution, we computed the mean rate over all branches assigned to a given clade, weighted by the length of the branch.

We developed visualization software for plotting dynamic rate changes on phylogenetic trees. Our approach involves breaking each branch of the phylogeny into segments of length $\tau$, then computing evolutionary rates for each segment. Each sample from the posterior simulated with BAMM describes a potentially unique segment-specific macroevolutionary rate. Segments are then assigned colors based on the estimated mean rate value. For dynamic rate plots shown below, we set $\tau$ equal to 1% of the total tree depth. We refer to these phylogenetic rate visualizations as phylorate plots. Consensus phylorate plots were computed by averaging segment-specific rates for each sample in the posterior distribution of rate shift configurations simulated with BAMM. This enables us to approximate the marginal density of evolutionary rates at any location in a phylogenetic tree.

### *Rates of Species Diversification*

We used BAMM to estimate rates of speciation and extinction across the sphenomorphine phylogeny (Rabosky 2014). The general model is similar to that described above for phenotypic evolution and assumes that phylogenetic trees may have been shaped by a heterogeneous mixture of distinct evolutionary regimes of speciation and extinction. As in Rabosky (2014) we allowed each regime to be characterized by a distinct time-varying speciation process such that the speciation rate $\lambda$ varies exponentially through time. This exponential change model has been widely used in diversification studies (Rabosky and Lovette 2008) and also is expected to provide a reasonable approximation to diversity-dependent changes in speciation rates through time (Quental and Marshall 2009). We assumed that the extinction rate $\mu$ is constant through time within regimes. However, we avoid interpreting extinction rates because of substantial controversy over the meaning of this parameter as estimated from molecular phylogenies (Quental and Marshall 2010; Rabosky 2010; Morlon et al. 2011; Quental and Marshall 2011; Etienne et al. 2012) and because a primary focus of this paper is on the relationship between speciation and morphological evolution. We accounted for incomplete taxon sampling using the analytical correction developed in several earlier studies (Nee et al. 1994; Yang and Rannala 1997; FitzJohn et al. 2009), as implemented in BAMM (Rabosky et al. 2013; Rabosky 2014). We assumed that our sampling included 86% of extant sphenomorphine skink diversity. To account for the effects of phylogenetic uncertainty on our analyses, we conducted BAMM analyses of phenotypic evolution and species diversification across 500 trees sampled from the posterior distribution of topologies and branch lengths.

### *Analysis and Interpretation of Rate Shifts*

Stepwise approaches for identifying macroevolutionary rate shifts on phylogenetic trees typically report a single optimal set of shift locations on a phylogenetic tree. Perhaps, the most significant limitation of these methods is that they frequently confound evidence for the number of rate shifts with evidence for the location of the rate shifts. In a typical stepwise analysis, model complexity is increased until some optimal number of shifts is found. The maximum likelihood shift configuration is reported, but evidence favoring this shift configuration over alternative shift configurations with equal numbers of parameters is rarely presented. However, other sets of rate shifts might be nearly as probable as the maximum likelihood estimate (MLE).

To address this issue, we introduce the concept of "distinct shift configurations." A distinct shift configuration is a realized history of diversification that is actually sampled during simulation of the posterior. Formally, we can describe each sample from the posterior simulated with BAMM by a set of topological locations (branches) on which rate shifts are observed to occur. The total number of distinct shift configurations is simply the number of such sets that account for all samples in the posterior.

Consider the example shown in Figure 3. Here, we illustrate a sister-clade relationship between a high-diversity clade (X) and a low-diversity clade (Y). This pair of clades (X, Y) is in turn sister to a clade of intermediate diversity (Z). A BAMM analysis of this data set might reveal two distinct shift configurations that explain the data: either diversification rates increased in the stem lineage leading to clade X (with $P = 0.6$), or rates have decreased along the lineage leading to clade Y (with $P = 0.4$). The probability of observing either shift is 1.0 (all samples in the posterior have one of these two shifts), yet no samples have both shifts. For this simple example, it is possible to enumerate all distinct shift configurations observed in the posterior, as well as their frequencies

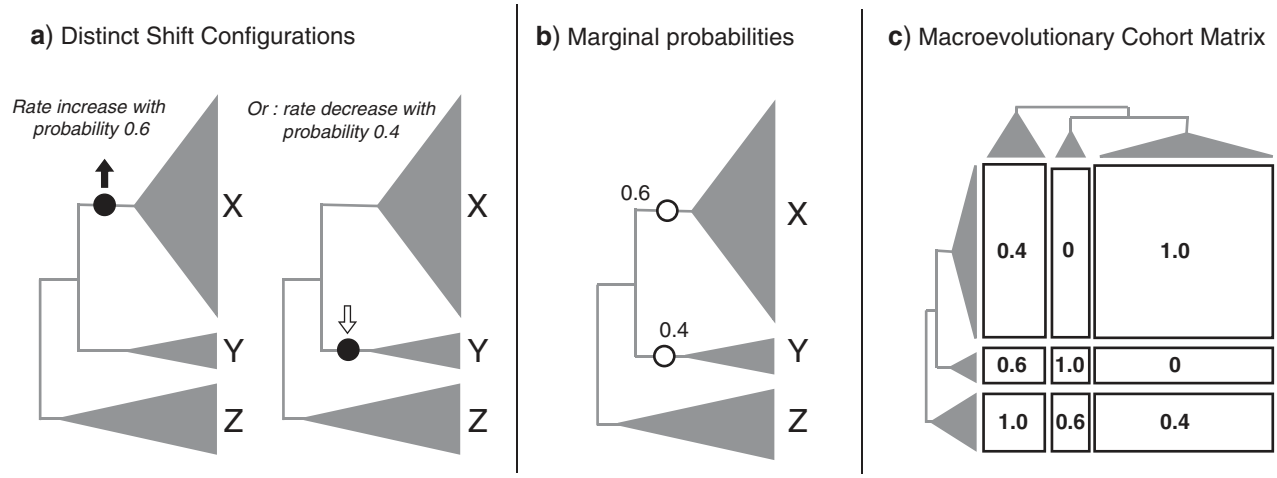


FIGURE 3. Hypothetical analysis of a single phylogenetic tree with BAMM to illustrate conceptual challenges in the interpretation of rate shifts on phylogenetic trees. Model tree includes a species-rich (X) and species-poor (Y) clade. (a) BAMM samples exactly two distinct shift configurations during simulation of the posterior: a diversification rate increase on the branch leading to clade X ($P=0.6$), or a rate decrease on the branch leading to clade Y ($P=0.4$). Every sample in the posterior includes one of these two shifts, but no sample has both. (b) Marginal shift probabilities on individual branches displayed on a single phylogenetic tree. (c) Macroevolutionary cohort matrix for this example. Clades X, Y, and Z define a $3\times3$ matrix, where each cell depicts the pairwise probability that two clades share a common macroevolutionary rate regime. For reference, the phylogeny is shown to the right and top of the matrix. From (a), all species in clade X share a common rate dynamic, and the same is true for clades Y and Z. Clades X and Y never share a common rate dynamic, because their dynamics are decoupled by the occurrence of a rate shift on one of the ancestral branches. The shift configurations depicted in (a) further specify the probability that clades X and Y share a common dynamic with clade Z.

(Fig. 3a). A typical stepwise AIC-based analysis would identify only the shift on the branch leading to clade X, despite the fact that this shift location is only weakly favored over the alternative shift configuration.

It is also possible to display marginal shift probabilities associated with each branch within a single phylogenetic tree (Fig. 3b). However, this plot fails to convey the overall probability that a rate shift occurred somewhere in the tree ($P=1.0$), as well as the negative correlation between the two observed shift locations (e.g., two shifts are never observed together in the same sample).

We developed an alternative method of summarizing diversification histories that avoids some of the challenges associated with enumerating and interpreting all distinct shift configurations (Fig. 3a) as well as displaying marginal probabilities for all rate shifts on a single phylogeny (Fig. 3b). This approach, which we refer to as macroevolutionary cohort analysis, depicts the pairwise probability that any two lineages or clades share a common set of macroevolutionary rate parameters (Fig. 3c); note phylogeny for reference on the left and upper margins of the matrix. For a given sample from the posterior distribution simulated with BAMM, a pair of species is assigned a value of 1 if they inherit a common rate dynamic and a value of 0 if they have different rate dynamics. A mean value is then computed over the full set of sampled shift configurations in the posterior distribution. A value of 0.5 implies that 50% of the samples in the posterior distribution include the focal species within a common macroevolutionary rate regime. These pairwise probabilities can even be averaged across posterior distributions of phylogenies to accommodate phylogenetic uncertainty. Note that any two species can share a common rate dynamic even if no rate shifts are present, because they would then share the same root process (Fig. 2a). We applied all three approaches illustrated in Figure 3 to visualize and interpret diversification shifts across the sphenomorphine skink radiation.

### *Software Availability*

BAMM is a C++ command line program that is freely available at www.bamm-project.org and licensed under GPL 2.0. All visualization was performed using R and C code available through the R package BAMMtools, a comprehensive set of tools for processing and visualizing BAMM output. BAMM source code, R functions and sample workflows for analyses described here are included in the Dryad data bundle that accompanies this publication.

## RESULTS

### *Phylogenetics of Australian Sphenomorphines*

We found strong support for the monophyly of the species-rich genus *Ctenotus* (Fig. 4; Appendix 1, http://doi.org/10.5061/dryad.kd38f). This result is consistent with previous findings (Rabosky et al. 2007; Skinner et al. 2013), but the results we report here are based on greatly expanded taxonomic coverage of the genus. In addition, the genus *Lerista* was found to be monophyletic, a result that is also consistent

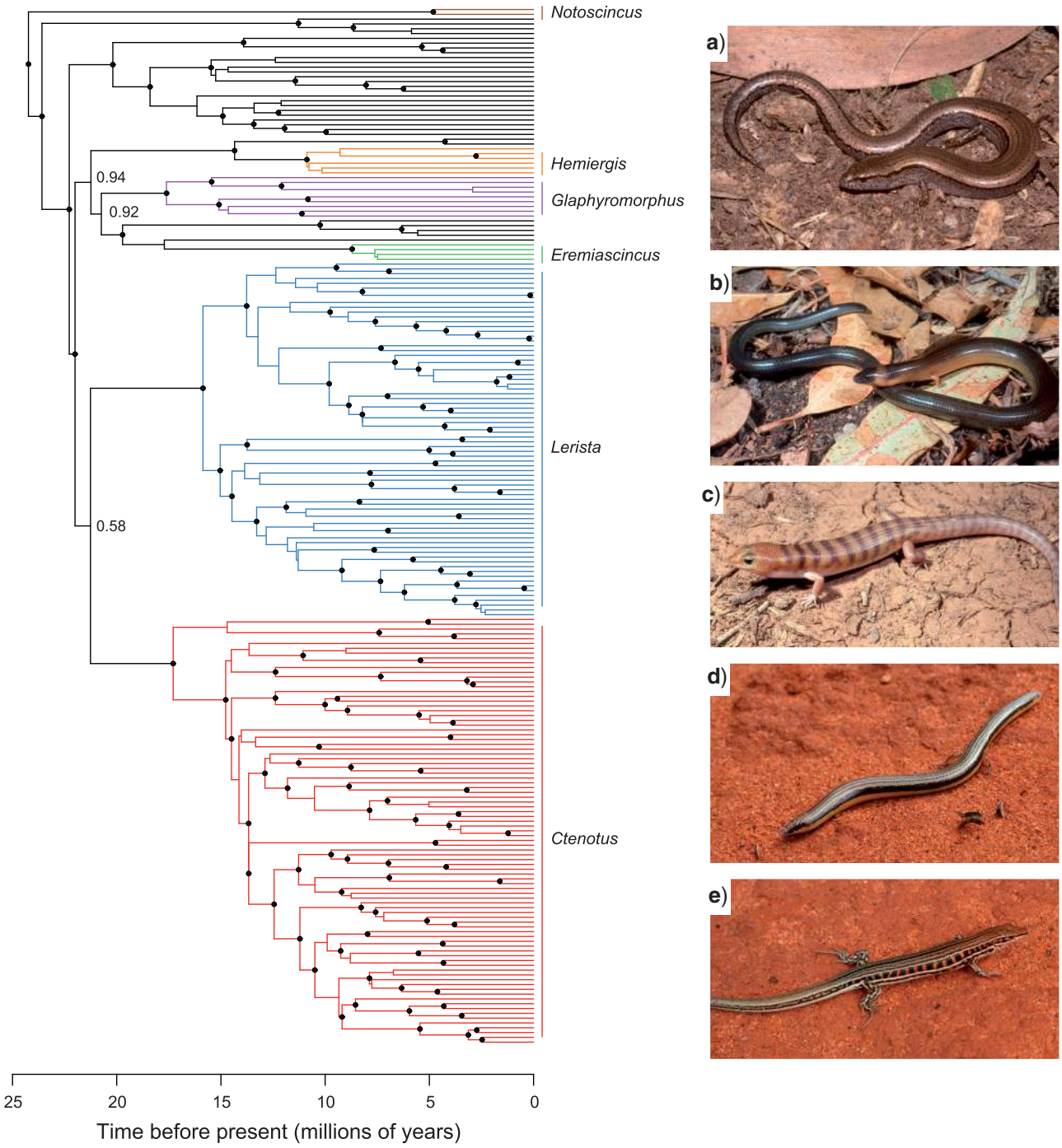


FIGURE 4. MCC tree for 216 species of Australian sphenomorphine skinks from Bayesian analysis of concatenated mitochondrial and nuclear DNA. Filled circles on nodes denote posterior probabilities >0.95; posterior probabilities for several key nodes with reduced support are also shown. Not all genera are labeled (Appendix 1, http://doi.org/10.5061/dryad.kd38f). Images show representative sphenomorphines: (a) *Hemiergis decresiensis*; (b) *Anomalopus verreauxii*; (c) *Eremiascincus richardsonii*; (d) *Lerista picturata*; and (e) *Ctenotus schomburgkii*. Photographs by M.N. Hutchinson (a, b, and c) and D.L. Rabosky (d and e).

with previous studies (Skinner et al. 2008). We find weak support (posterior probability = 0.58) for a sister clade relationship between *Lerista* and *Ctenotus*. Several other genera may not be monophyletic (*Anomalopus*, *Glaphyromorphus*, and *Eulamprus*), as suggested by previous studies (Skinner et al. 2013). The 95% credible interval on the crown age of *Ctenotus* was estimated to range from 13.7 to 23.3 Ma, and the corresponding interval for *Lerista* ranged from 12.9 to 22.1 Ma.

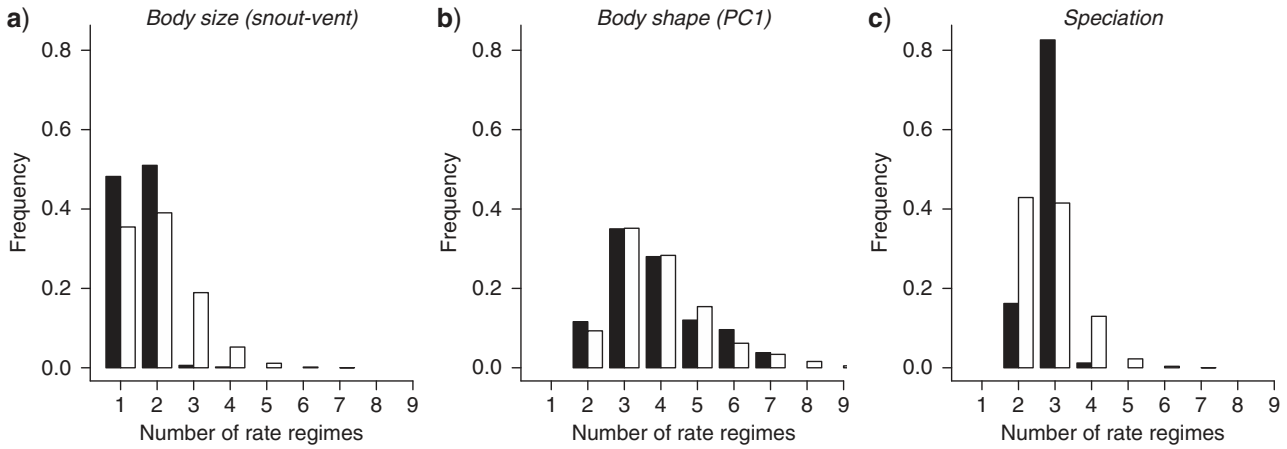


FIGURE 5. Marginal distributions of the number of distinct macroevolutionary rate regimes present in the sphenomorphine skink data set for (a) rates of body size evolution, (b) rates of body shape (PC1) evolution, and (c) rates of speciation. Results are shown for the MCC tree considered separately (white bars) and for a sample of 500 phylogenies taken from their posterior distribution (black bars). The posterior probability of a given model (e.g., a model with a particular number of regimes) is proportional to the frequency with which the model is sampled using reversible jump MCMC. A model with a single rate regime has zero rate shifts. For body size, models with one and two regimes have similar posterior probabilities, suggesting that clades do not differ appreciably in the dynamics of body size evolution. In contrast, the best-fit model of body shape evolution involves at least two distinct rate regimes and implies that one or more subclades underwent a shift in the dynamics of phenotypic evolution. Similar results are observed for speciation, where a model with a single rate regime has extremely low posterior probability (c). Rates (speciation and phenotypic evolution) are not assumed to be constant through time within a particular regime. Posterior odds ratios for any pair of models can be computed as the ratio of the posterior densities shown above.

### *Number of Macroevolutionary Regimes*

We conducted BAMM analyses across 500 time-calibrated phylogenies taken from the posterior distribution of topologies and branch lengths sampled with BEAST. From these results, we estimated the marginal density of the number of distinct macroevolutionary regimes that occurred in the sphenomorphine data set for body size, body shape, and speciation (Fig. 5). We found little evidence for multiple regimes in the evolutionary dynamics of skink body sizes (Fig. 5a). Across 500 phylogenies taken from the posterior distribution of topologies and branch lengths sampled with BEAST, the median posterior probability of a model with a single regime was 0.40. Only four of the 500 phylogenies (<1%) showed substantial evidence (total posterior probability >0.95) for more than one evolutionary rate regime in body size.

In contrast, rates of body shape evolution (PC1) varied substantially among clades (Fig. 5b). A three-regime model was favored by the majority of phylogenetic trees in the posterior distribution (0.025 and 0.975 quantiles of two and seven regimes). A single process model was rejected for all 500 phylogenies (single process model posterior probability <0.001 for all trees). The posterior probability of a two-process model was less than 0.05 for more than half of all trees (270 of 500). Across the full sample of phylogenies, the posterior odds ratio in favor of model with three regimes over a model with two regimes was 3.01. For speciation (Fig. 5c), the median number of rate regimes was 3, with 0.025 and 0.975 quantiles of two and three regimes. Across all 500 phylogenies, the model with the highest posterior probability contained at least two rate regimes. For all but 14 phylogenies (97.2%), a model with a single process had a posterior probability less than 0.05. These results provide strong evidence for among-clade heterogeneity in the dynamics of both body shape evolution and speciation, but not body size evolution.

### *Evolutionary Rate Dynamics*

We estimated the marginal Bayesian posterior densities of macroevolutionary rates in *Lerista* and *Ctenotus* relative to the mean rates in other Australian sphenomorphine skinks. For each tree in the posterior distribution that was analyzed with BAMM, a relative rate was computed as the ratio of the average macroevolutionary rate in *Lerista* or *Ctenotus* to the corresponding mean rate across all other (non-*Ctenotus* and non-*Lerista*) lineages. Mean rates for each clade were simply the mean marginal rates across all branches in the clade weighted by branch length. To estimate the mean rate for non-*Lerista*, non-*Ctenotus* lineages, we restricted calculations to branches that were coeval in time with the *Lerista*/*Ctenotus* radiations, and thus reducing the effects of overall temporal trends in evolutionary rates across the entire sphenomorphine radiation.

Results for body size (Fig. 6a) indicate that rates of body size evolution in both clades are similar to each other, but that these rates are slightly lower (~60–90%) than the mean rate of body size evolution in other lineages. In contrast, rates of body shape (PC1) evolution differ profoundly between *Lerista*, *Ctenotus* and other skink lineages, with *Ctenotus* undergoing an approximate 10-fold decrease in mean shape evolutionary rate (Fig. 6b). Rates of speciation in both *Ctenotus* and *Lerista* (Fig. 6c) are substantially elevated

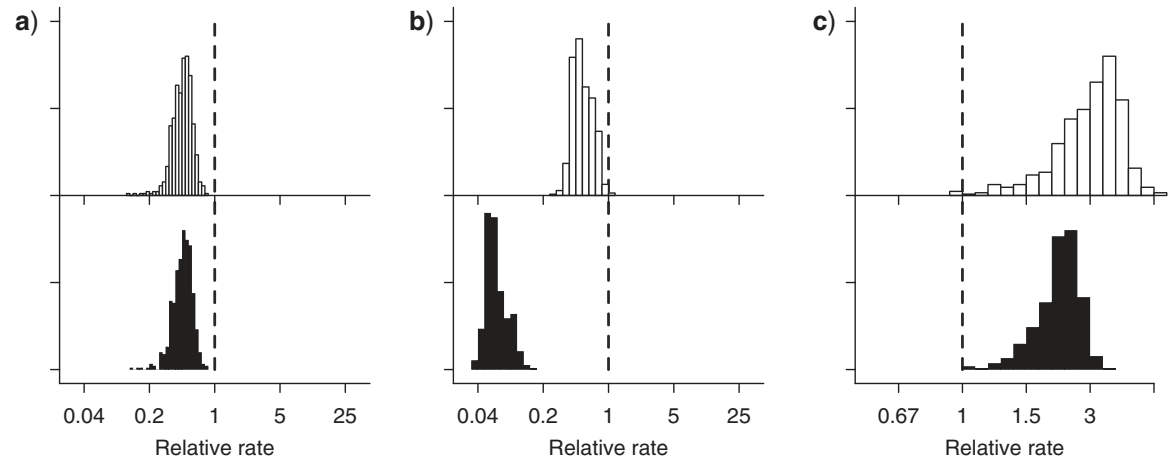


FIGURE 6. Marginal densities of macroevolutionary rates in *Lerista* (top; white) and *Ctenotus* (bottom; black) relative to the background rates observed across other sphenomorphine skink lineages. Shown are results for (a) the rate of body size evolution, (b) the rate of body shape evolution, and (c) the rate of speciation. These relative rates were estimated by dividing the mean marginal rate computed from all *Ctenotus* (or *Lerista*) lineages by the mean marginal rate across all non-*Ctenotus*, non-*Lerista* lineages. A relative rate of 1.0 implies equality of rates between *Lerista* or *Ctenotus* and all other sphenomorphine skink lineages. For body shape, *Ctenotus* has undergone a massive reduction in the rate of morphological change relative to *Lerista* as well as all other sphenomorphine skink lineages. For speciation, both clades have relative rates that are substantially faster than the background rate. Because all BAMM analyses were conducted across a sample of phylogenies from their posterior distribution, the variance in relative rate estimates reflects both phylogenetic uncertainty in relative rates as well as parametric uncertainty in model parameters.

relative to the background sphenomorphine rate. The mean of the posterior distributions of speciation rate for *Ctenotus*, *Lerista*, and other lineages are 0.137, 0.162, and 0.104 lineages/myr, respectively. The mean relative increase in speciation rate for *Ctenotus* was 1.32 (95% credible interval: 0.90–1.56) and the corresponding value for *Lerista* was 1.59 (95% credible interval: 0.87–2.14).

We visualized rate-through-time dynamics for speciation and phenotypic evolutionary rates for *Ctenotus*, *Lerista*, and "other" sphenomorphine lineages (Fig. 7). The dynamics of body size evolution are relatively similar for all three groups (Fig. 7, top row). The modest difference between body size results presented in Figures 6 and 7 can partially be explained by the fact that rate estimates for Figure 6 incorporate the full posterior distribution of topologies and branch lengths sampled using BEAST, but results in Figure 7 depict only the results for the MCC tree. For body shape, the rate for *Ctenotus* quickly plunges to approximately zero, a decline that is clearly visible despite an overall strong trend toward declining rates of shape evolution across all other sphenomorphine lineages. For most of the history of the *Ctenotus* clade, observed rates of shape evolution are significantly lower than the background rate. In contrast, for the rate of speciation (Fig. 7, bottom), *Lerista* and *Ctenotus* both show rates that are significantly higher than the background rate for most of their history.

The evidence for declining rates of speciation within the sphenomorphines is not dependent on use of the BAMM model. The gamma statistic (Pybus and Harvey 2000) for the MCC sphenomorphine phylogeny is significantly less than expected under a constant-rate diversification process ($\gamma = -9.64$; $P < 0.0001$ from simulation assuming 86% taxon sampling). This value of gamma remains significant even if we assume that the true number of species in the clade is much higher than currently recognized. For example, if the total diversity of sphenomorphines is 500 (implying 250 yet-unknown species), the observed value of gamma remains much lower the 0.05 percentile of the null distribution derived from constant rate simulations ($\gamma_{0.05} = -4.82$).

### *Analysis and Visualization of Rate Shifts*

We estimated the number of distinct shift configurations for species diversification and body shape evolution. We do not present results for body size evolution, because a model with zero rate shifts (e.g., one distinct process: the root process) was the most frequently sampled distinct shift configuration. The number of distinct shift configurations is usually large under the BAMM model. However, most shifts will have extremely low marginal probabilities: the BAMM model leads to a high frequency of ephemeral shifts that are proposed and accepted during simulation of the posterior that subsequently drop off after some number of generations as they fail to increase the posterior probability of the model sufficiently to justify their retention. Hence, we ignored all shifts with marginal probabilities less than 0.01 during the enumeration of distinct shift configurations (Supplementary Fig. S7, http://doi.org/10.5061/dryad.kd38f). The frequencies of the 10 most common shift configurations for phenotypic evolution and diversification are shown in Supplementary Figure S8, http://doi.org/10.5061/dryad.kd38f. For diversification (Supplementary Fig. S8b, http://doi.org/10.5061/dryad.kd38f), just

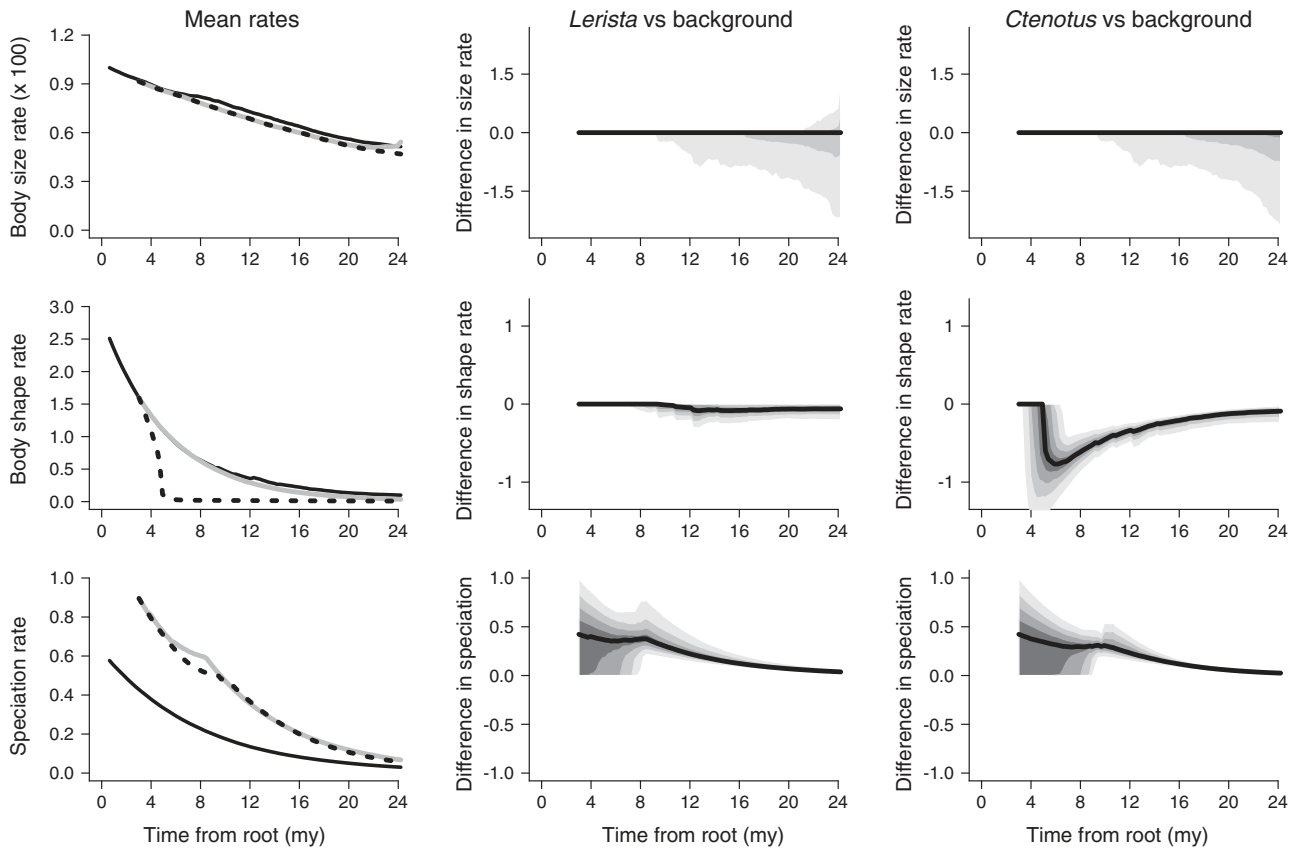


FIGURE 7. Temporal dynamics in rates of body size evolution (top row), body shape evolution (middle row), and speciation (bottom row) for Australian sphenomorphine skinks for the MCC tree. Left column shows overall mean rates through time for background lineages (black line) as well as for *Ctenotus* (dotted line) and *Lerista* (gray line). Middle column shows the difference, at any point in time, between the estimated *Lerista* rate and the estimated background rate, with gray polygons indicating the 0.10 to 0.90 quantiles on the distribution of rates (increments of 0.10). Median values are shown in black. Positive values indicate that the estimated rate exceeds the background rate at a particular point in time; negative values indicate that rates in the focal clade are slower than those in background lineages at a given point in time. Right-hand column shows corresponding curves for *Ctenotus*. In *Ctenotus*, the relative rate of body shape evolution dropped quickly to a level that was significantly below the background rate soon after the origin of the clade. In contrast, speciation rates in both *Ctenotus* and *Lerista* rise appreciably above the background rate. Rates of body size evolution for both *Ctenotus* and *Lerista* are indistinguishable from the background rate.

four distinct shift configurations account for 95% of the total probability of the data. For body shape evolution, 97 shift configurations are required to explain 95% of the data, although the vast majority have low probability. We note a potential point of confusion here: the frequency of a shift configuration can be lower than the marginal shift probability used to delimit distinct shift configurations; this is explained in Supplementary Figure S7, http://doi.org/10.5061/dryad.kd38f.

The four most common distinct shift configurations for body size evolution and diversification are shown in Figure 8, along with the corresponding consensus phylorate plots. The marginal shift probabilities for each branch are shown in Figure 9. The consensus phylorate plots are a summary of the marginal distribution of evolutionary rates at any time and topological location in a particular phylogeny. The *Ctenotus* clade has undergone a massive deceleration in the rate of body shape evolution, and this shift is clearly visible in the four most commonly sampled shift configurations. In fact, the marginal probability of a shift on the stem branch leading to *Ctenotus* is 0.95 (Fig. 9b).

For speciation, we also observe a high probability of regime shift associated with the origin of *Ctenotus* and *Lerista* (Fig. 8, bottom). The most frequently sampled shift configuration ($P = 0.56$) included a shift in the common ancestor of *Lerista* and *Ctenotus*, but no other shifts. The remaining three distinct shift configurations shown in Figure 8 include separate diversification shifts within *Ctenotus* and *Lerista*. Interestingly, when shifts occur separately within both *Ctenotus* and *Lerista*, we find little evidence for a distinct shift in evolutionary dynamics along the stem leading to the common ancestor of all extant *Ctenotus* lineages. Rather, the shift typically occurs along one of two basal branches within *Ctenotus* (Fig. 9c) and excludes a small species-poor *Ctenotus* clade (the *C. labillardieri* species group) consisting of several mesic taxa from southwestern Australia (*C. catenifer*, *C. delli*, *C. lancelini*, *C. gemmula*, and *C. labillardieri*: Appendix 1, Supplementary Figs. S4–S6,

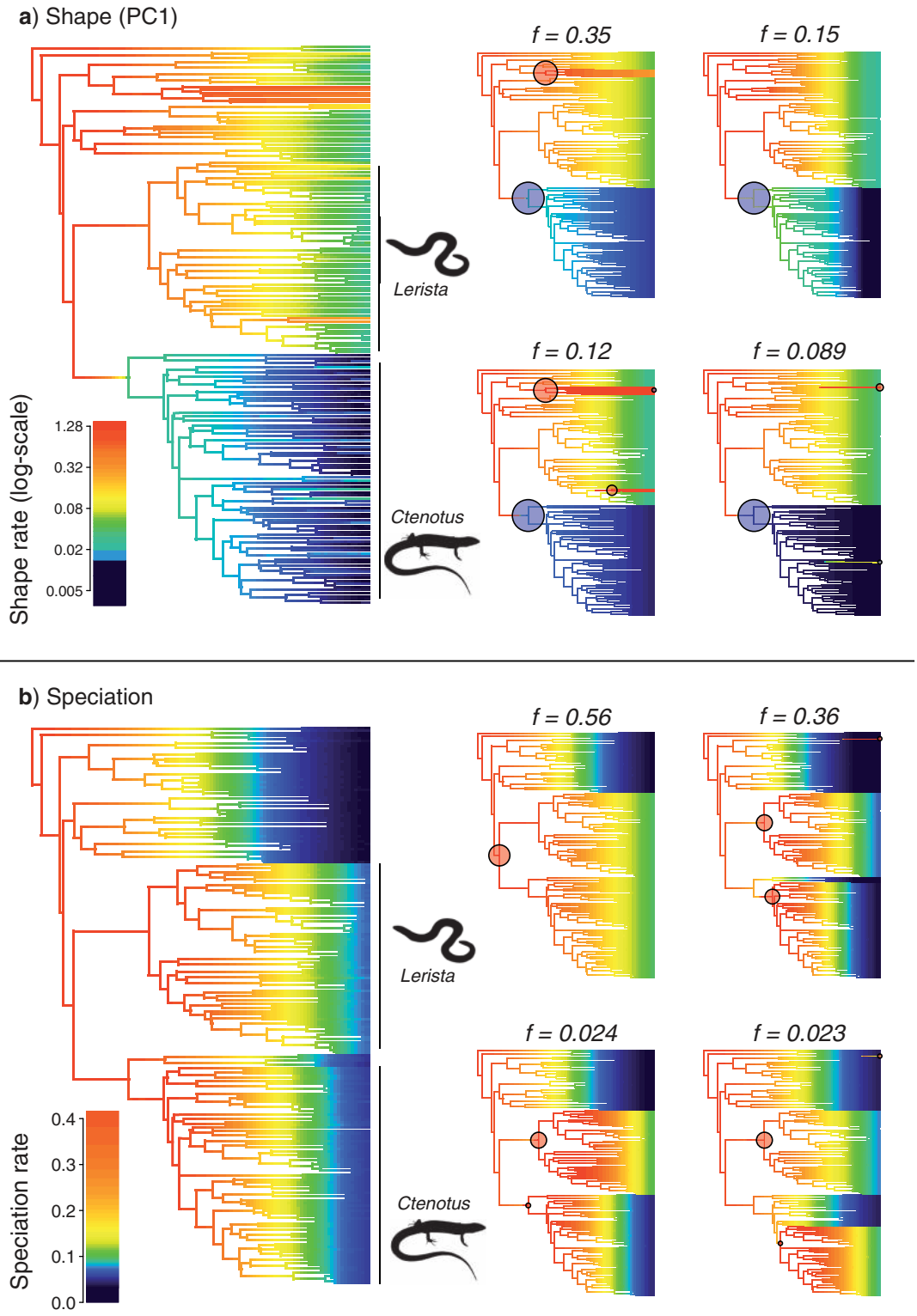


FIGURE 8. Phylorate plots for shape evolution (a) and speciation (b) using the MCC phylogeny; colors at each point in time along branches denote instantaneous rates of phenotypic evolution and speciation, respectively. Large trees (left side) depict "mean" phylorate plot, such that colors indicate the mean evolutionary rate across all shift configurations sampled during simulation of the posterior. Smaller phylogenies show the four distinct shift configurations with the highest posterior probability. For each distinct shift configuration, the locations of rate shifts are shown as red (rate increases) and blue (rate decreases) circles, with circle size proportional to the marginal probability of the shift. Text labels (e.g., $f = 0.35$) denote the posterior probability of each shift configuration. For body shape evolution, all four of the most common distinct shift configurations imply a massive deceleration in phenotypic rates along the branch leading to *Ctenotus*. For speciation, two distinct shift configurations account for most of the posterior probability of the data and imply either (i) a single rate shift in the immediate common ancestor of *Lerista* and *Ctenotus* ($P = 0.56$), or (ii) independent rate shifts in *Lerista* and the "core" *Ctenotus* clade ($P = 0.36$).

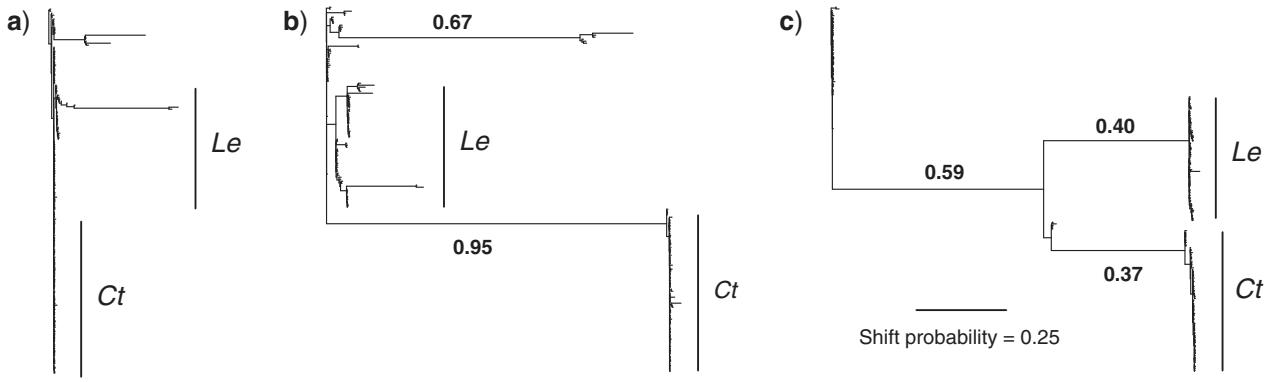


FIGURE 9. Marginal probabilities of rate shifts along any branch of the sphenomorphine MCC tree for body size (a), body shape (b), and speciation (c). Clades *Ctenotus* (Ct) and *Lerista* (Le) are labeled. For body size, there is little evidence for multiple regimes; hence, no single branch has strong support for a rate shift. In contrast, there is a high probability that a shift in the rate of body shape evolution occurred along the branch leading to *Ctenotus*. Branch-specific shift probabilities were computed independently for each branch and cannot be interpreted as the probability that a given clade has undergone a regime shift (Fig. 3). Moreover, there is little correspondence between marginal shift probabilities and the overall probability of rate heterogeneity. Note that the marginal shift probability of a particular node is not the same as the posterior probability of a particular "distinct shift configuration," because multiple distinct shift configurations may share particular shift locations. For example, all four configurations for body shape illustrated in Figure 8 contain a shift on the branch leading to *Ctenotus*.

http://doi.org/10.5061/dryad.kd38f). These results are clearly visible in the plot of marginal shift probabilities (Fig. 9c). The marginal probability of a single regime shift in the immediate ancestor of *Ctenotus* and *Lerista* is 0.59, but it is also possible that these clades have undergone independent increases in diversification (with $P = 0.40$). The conditional probability of at least one of these scenarios occurring, given this tree topology, is 0.97.

Macroevolutionary cohort matrices of BAMM results for body shape and diversification (Fig. 10) reveal numerous patterns that are difficult to visualize through consideration of distinct shift configurations (Fig. 8) or marginal shift probabilities (Fig. 9) alone. Plots for body shape and diversification reveal multiple distinct cohorts of lineages that are governed by common sets of macroevolutionary rate parameters. The MCC tree is shown for reference in the left and upper margins of Figure 9, but the color of each individual cell depicts the average correlation in rate regimes between two species averaged across the posterior distribution of phylogenies sampled using BEAST. We arbitrarily labeled major macroevolutionary cohorts of lineages identified through this analysis on the right margin (e.g., P1 and P2).

For body shape evolution (Fig. 10), it is immediately obvious that all species of *Ctenotus* can be grouped together as a well-supported cohort (P3). However, *Ctenotus* species show low correlations with all other sphenomorphine species. Most other sphenomorphine taxa show phenotypic rate dynamics that are highly correlated with other non-*Ctenotus* taxa (cohort P1), but a core block of six species has dynamics that are largely decoupled from all others (P2). This cohort is characterized by tremendous diversity of body form, including several typical forms with well-developed limbs (*Eulamprus tryoni* and *E. murrayi*), a robust and limbless form (*Coeranoscincus frontalis*), a slender nearly limbless form (*Ophioscincus truncatus*), and several species with considerable limb reduction (*Coeranoscincus reticulatus* and *Saiphos equalis*). The acceleration in rates for this cohort is clearly visible in the consensus phylorate plot for body shape as well as two of the four illustrated shift configurations (Fig. 8).

The macroevolutionary cohort matrix for diversification reveals highly correlated dynamics across non-*Ctenotus* and non-*Lerista* sphenomorphine species (labeled as S1). All *Lerista* species behave as a single well-supported cohort (S2), and dynamics in this group show very low correlations with cohort S1. Two cohorts are clearly defined within *Ctenotus*, including the species-poor *C. labillardieri* group (S3) and the remainder of the genus (S4). Interestingly, the S3 cohort shows dynamics that are more closely correlated with cohort S1 than with any other *Ctenotus* or *Lerista* species. With the exception of cohort S3, *Ctenotus* species are characterized by dynamics that are more correlated with those of *Lerista* (S2) than with any other sphenomorphine lineages (S1).

Results for body size reflect a lack of evidence for among-lineage heterogeneity in macroevolutionary rate dynamics. No single branch is associated with a high probability of regime shift (Fig. 9a), which is consistent with the high probability of a single rate regime for this data set (Fig. 5a). Supplementary Figure S11 (http://doi.org/10.5061/dryad.kd38f) shows the corresponding macroevolutionary cohort matrix for body size and clearly indicates that, on average, all species tend to share the same underlying macroevolutionary regime.

## DISCUSSION

We found strong support for heterogeneous macroevolutionary dynamics during the radiation of Australian sphenomorphine skinks. Using a new

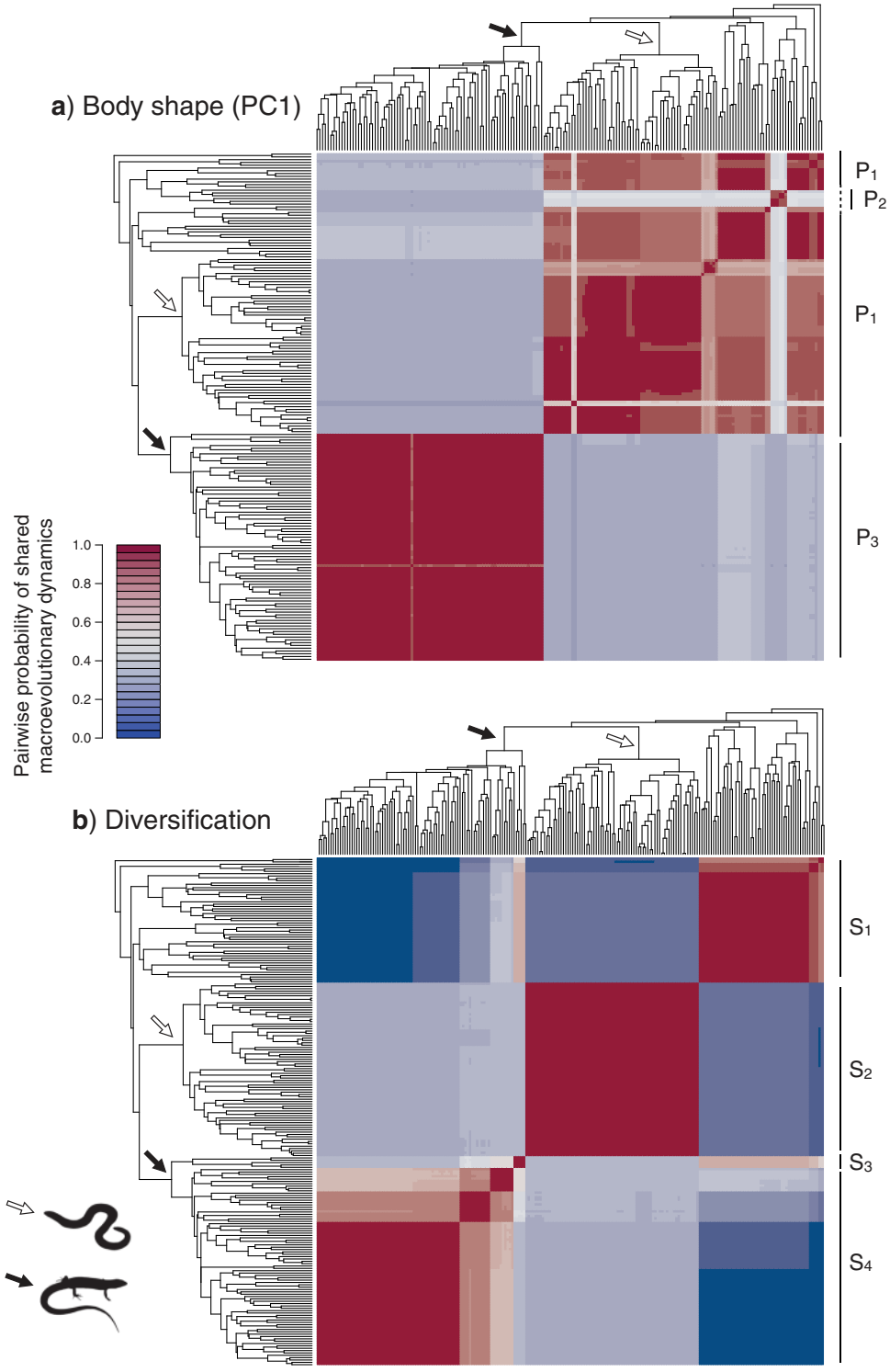


FIGURE 10. Macroevolutionary cohort matrices for body shape (a) and speciation (b) in Australian sphenomorphine skinks. Each cell in the matrix (a: 183 × 183; b: 216 × 216) is coded by a color denoting the pairwise probability that two species share a common macroevolutionary rate regime. The MCC phylogeny is shown for reference on the left and upper margins of each cohort matrix, but pairwise probabilities are averages from BAMM analyses conducted over a sample of trees from the posterior distribution of topologies and branch lengths. Major cohorts of taxa that tend to share common rate dynamics are labeled on the right margin of the plot. For body shape (a), it is immediately obvious that all *Ctenotus* species have highly correlated rate dynamics (regime P3). Likewise, most other sphenomorphine taxa are characterized by (largely) shared rate dynamics (P1), with the exception of a small block of taxa with their own rate dynamic (P2). For speciation, at least four major cohorts can be identified: S1, "core" *Ctenotus*; S2, *Ctenotus labillardieri* clade; S3, *Lerista*; S4, other sphenomorphines. Compare macroevolutionary cohorts with phylorate plots in Figure 8.

Bayesian approach for quantifying complex mixtures of evolutionary processes on phylogenetic trees (BAMM), we found that rates of body shape evolution and speciation varied both among lineages and through time during the sphenomorphine skink radiation.

### *Macroevolutionary Rate Variation among Lineages*

The rate of body size evolution appears to differ between skink lineages (Fig. 6a), as *Ctenotus* and *Lerista* appear to have reduced rates of size evolution relative to the background rate. However, these rate differences pale in comparison with variation in the rate of shape evolution (Figs. 6b and 7). The dynamics of shape evolution in the *Ctenotus* clade are distinct from dynamics in other sphenomorphine lineages. It is most likely that this pattern reflects a discrete shift in the mode of body shape evolution in the common ancestor of *Ctenotus* (Figs. 8 and 9c). In some respects, these results are unsurprising, given the markedly reduced variation in body shape for *Ctenotus* relative to other sphenomorphines (Fig. 1).

Our results provide insight into alternative evolutionary scenarios that may have generated the observed distribution of body shape across sphenomorphines. The marginal probability of a rate shift on the branch leading to Ctenotus is 0.95 (Fig. 9c), but it is also possible that *Ctenotus* merely inherited a low ancestral rate (with $P = 0.05$). However, this scenario then requires that multiple other sphenomorphine lineages underwent independent increases in the rate of shape evolution. This latter scenario is less probable and requires an increase in the number of distinct evolutionary regimes to explain the data. Supplementary Figure S11 (http://doi.org/10.5061/dryad.kd38f) shows the posterior distribution of the number of evolutionary regimes in body shape evolution, conditional on a shift occurring (Supplementary Fig. S11a, http://doi.org/10.5061/dryad.kd38f) or not occurring (Supplementary Fig. S11b, http://doi.org/10.5061/dryad.kd38f) along the branch leading to the *Ctenotus* clade. The distribution shifts markedly if no shift occurs on the *Ctenotus* branch, because this scenario then requires multiple independent increases in the rate of shape evolution on at least four other branches. Although the four most frequently sampled distinct shift configurations (Fig. 8) contain a rate decrease on the branch leading to *Ctenotus*, several shift configurations that do not include a shift on this branch can be seen in an expanded plot of the 20 most frequently sampled shift configurations (Supplementary Fig. S9, http://doi.org/10.5061/dryad.kd38f). The ability to visualize alternative scenarios of evolutionary change by conditioning (e.g., shift occurs or does not occur on the stem *Ctenotus* branch) is a major advantage of the BAMM framework relative to other methods.

At most points in time, speciation rates for both *Ctenotus* and *Lerista* exceed the corresponding rate for contemporaneous background lineages (Fig. 7, bottom row). The relative rate differences shown in Figure 6 are on the order of 1.5; left unchecked, such a difference can lead to massive disparities in species richness among clades. Indeed, under a pure-birth process, the expected ratio of species richness in sister clades with a relative rate difference of $k$ is equal to $\exp((k-1)\,\lambda T)$, where $T$ is the crown age of clades and $\lambda$ is the speciation rate in the clade with the lower rate. However, it is unlikely that species richness ever increases in unconstrained, unbounded fashion (Sepkoski 1978; Rosenzweig 1995; Alroy 2010a, 2010b; Etienne and Haegeman 2012; Etienne et al. 2012; Rabosky 2013), due to diversity-dependent regulation of speciation and/or extinction rates. Despite a large increase in speciation rates in *Ctenotus* and *Lerista*, all lineages are characterized by strong temporal decelerations in the rate of speciation.

### *Relationship between Speciation and Morphological Evolution*

We find no evidence that high rates of morphological evolution are associated with high rates of speciation. The genus *Ctenotus* is perhaps the most species-rich vertebrate genus in Australia and has undergone rapid species diversification (Fig. 6c). However, this pattern of speciation is not associated with an increase in the rate of evolution of body size and shape. The discrepancy with body shape evolution is particularly striking, because rates of shape evolution in *Ctenotus* have effectively dropped to zero (Fig. 8). This result suggests that speciation in sphenomorphine skinks is not associated with divergence along the major axis of phenotypic variation summarized by PC1 from our morphometric analyses. This principal component appears to be a general measure of limb reduction and body elongation. Most taxa that show clear evidence for both elongation and limb reduction have high scores on PC1, such as the genus *Anomalopus* (PC1 range for measured species: 3.6–7.6; $n = 5$), *Lerista* (PC1 range: −0.4 to 7.5, $n = 63$), and *Coeranoscincus* (PC1 range: 0.5–7.3, $n = 2$). In contrast, *Ctenotus* species score low on PC1 and show little variation overall (range: −2.3 to −0.7, $n = 82$; Fig. 1).

Evolutionary lability of form and function is sometimes considered to be a key innovation that can promote species diversification (Vermeij 1973; Liem and Osse 1975; Lovette et al. 2002). Our results suggest that this model does not apply to size and shape in sphenomorphine skinks. Overall rates of both size and shape evolution in both *Lerista* and *Ctenotus* are not correlated with rates of speciation. *Ctenotus* has been able undergo a dramatic decrease in the tempo of body shape evolution while retaining a fast overall rate of species diversification. These results contrast with those reported in several recent phylogenetic studies, which found that rates of morphological evolution were correlated with species diversification (Rabosky and Adams 2012; Rabosky et al. 2013).

It is possible that evolutionary rates of other phenotypic traits are correlated with elevated speciation rates in *Lerista* and *Ctenotus*. For example, previous studies have suggested that rates of climate niche evolution are associated with elevated diversification rates (Kozak and Wiens 2010). This is possible and receives some anecdotal support. Most non-*Ctenotus*, non-*Lerista* lineages of sphenomorphine skinks are restricted to higher rainfall regions of Australia. *Lerista* and *Ctenotus* are noteworthy for their exceptional species richness in the arid regions of Australia (Greer 1989; James and Shine 2000; Rabosky et al. 2007), but it is also true that many species from both clades occur in other climatic regions. Phenotypic lability in *Lerista* and *Ctenotus* may also be high along ecological axes that are not correlated with body size and general shape. *Ctenotus*, for example, shows high evolutionary lability of macrohabitat use within regional communities (Rabosky et al. 2011). Other ecological niche axes do not appear to be especially labile: diet appears to be more conserved across *Ctenotus* than across several other clades of arid-zone lizards (Rabosky et al. 2011), although individual species may still show relatively low overlap in diet (Goodyear and Pianka 2011).

### *Evolution of Australian Skinks*

Perhaps the most striking result from our analyses is the dramatic shift in morphological evolution associated with the *Ctenotus* clade (Figs. 7 and 8). Why has this group undergone such a dramatic decrease in rates of body shape evolution? Some insight into this question comes from considering the ecology of non-*Ctenotus* lineages of sphenomorphine skinks. Most species with extensive limb reduction (e.g., species in the genera *Lerista*, *Anomalopus*, *Coeranoscincus*, and *Ophioscincus*) are burrowing animals. Even lineages with lesser degrees of limb reduction (e.g., *Hemiergis*) or no limb reduction (*Gnypetoscincus*) tend to live under cover in relatively moist environments. *Ctenotus* species, in contrast, are decidedly non-fossorial: they are not cover restricted and are, for the most part, active and wide-ranging diurnal foragers (Pianka 1969). *Ctenotus* also appears to have undergone a shift in thermal ecology relative to many other sphenomorphines (Garland et al. 1991) and both tolerates and prefers high active body temperatures. We suggest that *Ctenotus* has undergone a fundamental and adaptive ecological shift that has enabled it to occupy a broad range of terrestrial, non-fossorial ecological niches that are not used by other sphenomorphine skink lineages.

Other explanations for the patterns observed in *Ctenotus* are possible. For example, the ancestor of *Ctenotus* might have lost the capacity to evolve elongate and limb-reduced forms. However, in light of the clear ecological differences between *Ctenotus* and other sphenomorphines, we feel that it is unlikely that these patterns reflect a shift in the underlying developmental-genetic architecture of limb reduction in the common ancestor of *Ctenotus*. Had the lineage leading to *Ctenotus* merely lost ability to undergo body elongation and limb reduction, we would have had little reason to expect elevated rates of species diversification in the group. The coupling of a modal shift in shape evolution with high speciation rates suggests the possibility that the *Ctenotus* lineage has diversified within an adaptive zone that is distinct from that occupied by other sphenomorphine lineages. Nonetheless, it is possible that several factors have acted in concert to explain the nearly compete absence of body elongation and limb reduction in *Ctenotus*.

### *Visualization and Analysis of Complex Macroevolutionary Dynamics*

The BAMM framework we have developed is able to simultaneously model phenotypic rate variation both among lineages and through time. Because we could reconstruct marginal distributions of evolutionary rates at any point in time along any branch of the sphenomorphine tree, we were able to reconstruct relative rate differences through time for the *Ctenotus* and *Lerista* clades relative to all other sphenomorphine lineages. As such, BAMM is fundamentally different from other multi-model approaches for studying macroevolutionary dynamics. For example, the MEDUSA model (Alfaro et al. 2009) allows rates of speciation and extinction to vary among clades, but assumes that rates are constant through time within a particular regime. Likewise, several recent Bayesian approaches for detecting among-clade variation in phenotypic evolutionary rates assume rate-constancy through time, (Eastman et al. 2011; Revell et al. 2012), although there is no reason in principle why these models could not be extended to model rate variation through time as we have done here. Our results for both trait evolution and speciation strongly reject time-constant rates for sphenomorphine skinks: both trait evolution and speciation show strong temporal trends that are unrelated to clade-specific differences in rates. We also demonstrated how BAMM analyses could be performed across distributions of phylogenetic trees to account for uncertainty in both phylogenetic topology and branch lengths (Figs. 5, 6, and 10).

The methods and software developed here enabled us to characterize sets of distinct shift configurations that could plausibly give rise to the observed data (Figs. 3 and 8; Supplementary Fig. S7, http://doi.org/10.5061/dryad.kd38f). Traditional approaches for studying rate shifts on phylogenetic trees provide researchers with the equivalent of a single MLE, with no information about the probability of the MLE relative to alternative shift configurations with equal numbers of shifts. As we have demonstrated (Figs. 7 and 8; Supplementary Figs. S8 and S9, http://doi.org/10.5061/dryad.kd38f), numerous distinct configurations of rate shifts can have fairly similar posterior probabilities. We suggest that researchers adopt a strategy of explicitly characterizing alternative shift configurations and their relative probabilities, rather than simply reporting a single

MLE shift configuration. For some data sets, it is likely that the MLE will be extremely well supported, as we observed for body shape evolution in the ancestor of *Ctenotus*. In this case, a single branch is associated with a high marginal shift probability. However, for many other data sets, we may have low confidence in any particular shift configuration, even if we are confident that rate heterogeneity occurs within our data set. For example, we have overwhelming evidence in favor of heterogeneous speciation dynamics across the sphenomorphine radiation, and the model with the highest posterior probability for all 500 phylogenies in our sample included at least two distinct macroevolutionary rate regimes. However, this probability is distributed somewhat equally across two distinct shift configurations (Fig. 8): either a single rate shift occurred in the common ancestor of *Lerista* and *Ctenotus*, or shifts occurred in both clades independently. It is worth pointing out that marginal shift probabilities (Fig. 9) are largely uninformative about the overall probability of rate heterogeneity across a data set.

Because of the difficult in visualizing large numbers of distinct shift configurations (Supplementary Fig. S8, http://doi.org/10.5061/dryad.kd38f), we introduced the concept of macroevolutionary cohort analysis (Figs. 3 and 10). This provides a summary of the extent to which any two species share a common macroevolutionary rate dynamic and can be averaged across posterior distributions of phylogenies to account for phylogenetic uncertainty. Macroevolutionary cohort matrices for body shape and diversification revealed sets of taxa that have diverged under common sets of rate parameters. The approach enables us to easily extract many features of diversification histories that would be invisible using MLEs. The approach also more accurately represents the covariation between evolutionary rate regimes that is obscured by examining marginal shift probabilities. For example, consider the marginal probability of a shift in diversification rates leading to the *Lerista* clade (Fig. 9c). From this figure, there is no way to assess the probability that a rate shift has decoupled the dynamics of *Lerista* diversification from those of other non-*Lerista*/non-*Ctenotus* lineages. The probability that a shift occurred on the branch leading to *Lerista* and *Ctenotus* is 0.59, and the probability of a shift on the *Lerista* stem branch is 0.40. Macroevolutionary cohort analysis (Fig. 10b) tells us that these shifts are negatively correlated, because the overall probability that *Lerista* speciation dynamics are decoupled from the background approaches 1.0. Hence, *Lerista* behaves as a unified macroevolutionary cohort with extremely high probability, even if we have considerable uncertainty over the precise branch on which the shift in dynamics occurred (Fig. 9c).

## Conclusion

A number of evolutionary models predict that rates of species diversification and morphological evolution should be coupled, but few phylogenetic tests of this relationship have been performed. We tested the relationship between speciation and phenotypic evolution during the radiation of Australian sphenomorphine skinks, a group of nearly 250 species of lizards that constitutes one of Australia's most species-rich vertebrate lineages. We generalized a recent multi-model Bayesian framework for modeling complex evolutionary dynamics (BAMM) to account for variation in macroevolutionary rates through time, thus simultaneously allowing both temporal and among-clade variation in evolutionary dynamics. Our results suggest that two clades (*Lerista* and *Ctenotus*) have undergone an acceleration in the rate of speciation relative to other sphenomorphine lineages. However, *Ctenotus* has undergone a massive deceleration in the rate of body shape evolution. This indicates that major axes of morphological variation can be decoupled from speciation during evolutionary radiations.

This decoupling of macroevolutionary dynamics contrasts with patterns observed in several other groups, including ray-finned fishes (Rabosky et al. 2013). The striking difference between the results we report here and those from Rabosky et al. (2013) raise questions about potential scale-dependence of the relationship between speciation and morphological evolution. Rabosky et al. (2013) considered rate-coupling across the entire actinopterygiian radiation (30,000+ species; crown age = 345 myr), whereas the present study assessed rate-coupling at a much smaller scale (~250 species; crown age = 25 myr). It is possible that rate-coupling would be observed across all squamate reptiles, but that the any such relationships are highly variable at much finer phylogenetic and taxonomic scales of analysis. Likewise, it is possible that squamates and ray-finned fishes differ fundamentally in the relationship between speciation and morphological evolution. Regardless, we have much to learn about the heterogeneous mixture of evolutionary processes that have shaped the distribution of species richness and phenotypic diversity across the sphenomorphine skinks.

## Supplementary Material

Data available from the Dryad Digital Repository: http://dx.doi.org/10.5061/dryad.kd38f.

## Funding

This work was supported by the Miller Institute for Basic Research in Science at the University of California and by National Science Foundation (NSF) grants OSIE-0612855, DEB-0814277 and DEB-1256330.

## Acknowledgements

The authors thank A.L. Talaba for assistance with DNA sequencing, P. Doughty for access to tissues, and F. Anderson, M. Cowan, P. Doughty, M. Hutchinson, A. Rabosky, V. Savolainen, G. Thomas, and an anonymous

reviewer for comments and discussion that improved the manuscript.

## References


Adamowicz S.J., Purvis A., Wills MA. 2008. Increasing morphological complexity in multiple parallel lineages of the Crustacea. Proc. Natl. Acad. Sci. U.S.A. 105:4786–4791.

Adams D.C., Berns C.M., Kozak K.H., Wiens J.J. 2009. Are rates of species diversification correlated with rates of morphological evolution? Proc. Biol. Sci. 276:2729–2738.

Alfaro M.E., Santini F., Brock C., Alamillo H., Dornburg A., Rabosky D.L., Carnevale G., Harmon L.J. 2009. Nine exceptional radiations plus high turnover explain species diversity in jawed vertebrates. Proc. Natl. Acad. Sci. U.S.A. 106:13410–13414.

Alroy J. 2010a. Geographical, environmental, and intrinsic biotic controls on Phanerozoic marine diversification. Paleontology 53:1211–1235.

Alroy J. 2010b. The shifting balance of diversity among major marine animal groups. Science 321:1191–1194.

Blomberg S.P., Garland T. Jr., Ives A.R. 2003. Testing for phylogenetic signal in comparative data: behavioral traits are more labile. Evolution 57:717–745.

Cheetham A.H. 1986. Tempo of evolution in a neogene bryozoan: rates of morphologic change within and across species boundaries. Paleobiology 12:190–202.

Darwin C. 1859. On the origin of species by means of natural selection. London: John Murray.

Drummond A.J., Rambaut A. 2007. BEAST: Bayesian evolutionary analysis sampling trees. BMC Evol. Biol. 7:214.

Eastman J.M., Alfaro M.E., Joyce P., Hipp A.L., Harmon L.J. 2011. A novel comparative method for identifying shifts in the rate of character evolution on trees. Evolution 65:3578–3589.

Eldredge N., Gould S.J. 1972. Punctuated equilibria: an alternative to phyletic gradualism. In: Schopf T.J.M., editor. Models in paleobiology. San Francisco (CA): Freeman Cooper. p. 182–215.

Etienne R.S., Haegeman B. 2012. A conceptual and statistical Framework for adaptive radiations with a key role for diversity dependence. Am. Nat. 180:E75–E89.

Etienne R.S., Haegeman B., Stadler T., Aze T., Pearson P.N., Purvis A., Phillimore A.B. 2012. Diversity-dependence brings molecular phylogenies closer to agreement with the fossil record. Proc. Biol. Sci. 279:1300–1309.

FitzJohn R., Maddison W.P., Otto S.P. 2009. Estimating trait-dependent speciation and extinction rates from incompletely resolved phylogenies. Syst. Biol. 58:595–611.

Garland T. Jr., Huey R.B., Bennett A.F. 1991. Phylogeny and coadaptation of thermal physiology in lizards: a reanalysis. Evolution 45:1969–1975.

Glor R.E. 2010. Phylogenetic insights on adaptive radiation. Ann. Rev. Ecol. Evol. Syst. 41:251–270.

Goodyear S.E., Pianka ER. 2011. Spatial and temporal variation in diets of sympatric lizards (genus *Ctenotus*) in the Great Victoria Desert, Western Australia. J. Herpetol. 45:265–271.

Greer A.E. 1989. The biology and evolution of Australian lizards. Chipping Norton (UK): Surrey Beatty and Sons.

Harmon L.J., Schulte J.A., Larson A., Losos J.B. 2003. Tempo and mode of evolutionary radiation in iguanian lizards. Science 301:961–964.

Heled J., Drummond A.J. 2010. Bayesian inference of species trees from multilocus data. Mol. Biol. Evol. 27:570–580.

Huelsenbeck J.P., Larget B., Swofford D. 2000. A compound Poisson process for relaxing the molecular clock. Genetics 154:1879–1892.

Hunt G. 2007. The relative importance of directional change, random walks, and stasis in the evolution of fossil lineages. Proc. Natl. Acad. Sci. U.S.A. 104:18404–18408.

Hunt G. 2008. Fitting and comparing models of phyletic evolution: random walks and beyond. Paleobiology 32:578–601.

Ingram T. 2011. Speciation along a depth gradient in a marine adaptive radiation. Proc. Biol. Sci. 278:613–618.

James C.D., Shine R. 2000. Why are there so many coexisting species of lizards in Australian deserts? Oecologia 125:127–141.

Kozak K.H., Wiens J.J. 2010. Accelerated rates of climatic-niche evolution underlie rapid species diversification. Ecol. Lett. 13:1378–1389.

Lemmon A.R., Moriarty E.C. 2004. The importance of proper model assumption in Bayesian phylogenetics. Syst. Biol. 53:265–277.

Liem K.F., Osse J.W.M. 1975. Biological versatility, evolution, and food resource exploitation in African cichlid fishes. Am. Zoologist. 15:427–454.

Liu L., Pearl D.K. 2007. Species trees from gene trees: reconstructing Bayesian posterior distributions of a species phylogeny using estimated gene tree distributions. Syst. Biol. 56:504–514.

Lovette I.J., Bermingham E., Ricklefs R.E. 2002. Clade-specific morphological diversification and adaptive radiation in Hawaiian songbirds. Proc. Biol. Sci. 269:37–42.

Mahler D.L., Revell L.J., Glor R.E., Losos J.B. 2010. Ecological opportunity and the rate of morphological evolution in the diversification of greater antillean anoles. Evolution 64:2731–2745.

Mattila T.M., Bokma F. 2008. Extant mammal body masses suggest punctuated equilibrium. Proc. Biol. Sci. 275:2195–2199.

Morlon H., Parsons T.L., Plotkin J.B. 2011. Reconciling molecular phylogenies with the fossil record. Proc. Natl. Acad. Sci. U.S.A. 108:16327–16332.

Nee S., May R.M., Harvey P.H. 1994. The reconstructed evolutionary process. Philos. Trans. R. Soc. Lond. B. Biol. Sci. 344:305–311.

Nosil P. 2012. Ecological speciation. New York: Oxford University Press.

Pennell M.W., Harmon L.J., Uyeda J.C. 2013. Is there room for punctuated equilibrium in macroevolution? Trends Ecol. Evol. 29:23–32.

Pfennig D.W., Pfennig K.S. 2013. Evolution's wedge: competition and the origins of diversity. Berkeley (CA): University California Press.

Pianka E.R. 1969. Sympatry of desert lizards (Ctenotus) in Western-Australia. Ecology 50:1012–1030.

Pigliucci M. 2008. Opinion—is evolvability evolvable? Nat. Rev. Genet. 9:75–82.

Pinto G., Mahler D.L., Harmon L.J., Losos J.B. 2008. Testing the island effect in adaptive radiation: rates and patterns of morphological diversification in Caribbean and mainland *Anolis* lizards. Proc. Biol. Sci. 275:2749–2757.

Price T. 2008. Speciation in Birds. Greenwood Village (CO): Roberts and Company.

Pybus O.G., Harvey P.H. 2000. Testing macro-evolutionary models using incomplete molecular phylogenies. Proc. Biol. Sci. 267:2267–2272.

Quental T.B., Marshall C.R. 2009. Extinction during evolutionary radiations: reconciling the fossil record with molecular phylogenies. Evolution 63:3158–3167.

Quental T.B., Marshall C.R. 2010. Diversity dynamics: molecular phylogenies need the fossil record. Trends Ecol. Evol. 25:434–441.

Quental T.B., Marshall C.R. 2011. The molecular phylogenetic signature of clades in decline. PLoS One 6:e25780.

Rabosky DL. 2010. Extinction rates should not be estimated from molecular phylogenies. Evolution 64:1816–1824.

Rabosky DL. 2012. Positive correlation between diversification and phenotypic evolvability can mimic punctuated equilibrium on molecular phylogenies. Evolution 66:2622–2627.

Rabosky DL. 2013. Diversity dependence, ecological speciation, and the role of competition in macroevolution. Ann. Rev. Ecol. Evol. Syst. 44:481–502.

Rabosky D.L. 2014. Automatic detection of key innovations, rate shifts, and diversity dependence on phylogenetic trees. PLoS One 9:e89543.

Rabosky D.L., Adams DC. 2012. Rates of morphological evolution are correlated with species richness in salamanders. Evolution 66:1807–1818.

Rabosky D.L., Cowan M.A., Talaba A.L., Lovette I.J. 2011. Species interactions mediate phylogenetic community structure in a hyperdiverse lizard assemblage from arid Australia. Am. Nat. 178:579–595.

Rabosky D.L., Donnellan S.C., Talaba A.L., Lovette I.J. 2007. Exceptional among-lineage variation in diversification rates during the radiation of Australia's most diverse vertebrate clade. Proc. Biol. Sci. 274:2915–2923.

Rabosky D.L., Lovette I.J. 2008. Explosive evolutionary radiations: decreasing speciation or increasing extinction through time? Evolution 62:1866–1875.

Rabosky D.L., Santini F., Eastman J.M., Smith S.A., Sidlauskas B., Chang J., Alfaro M.E. 2013. Rates of speciation and morphological evolution are correlated across the largest vertebrate radiation. Nat. Commun. 4:10.1038/ncomms2958.

Rabosky D.L., Talaba A.L., Donnellan S.C., Lovette I.J. 2009. Molecular evidence for hybridization between two Australian desert skinks, *Ctenotus leonhardii* and *Ctenotus quattuordecimlineatus* (Scincidae: Squamata). Mol. Phylogenet. Evol. 53:368–377.

Raia P., Carotenuto F., Passaro F., Piras P., Fulgione D., Werdelin L., Saarinen J., Fortelius M. 2013. Rapid action in the Paleogene, the relationship between phenotypic and taxonomic diversification in Coenozoic mammals. Proc. Biol. Sci. 280:20122244.

Reeder TW. 2003. A phylogeny of the Australian Sphenomorphus group (Scincidae: Squamata) and the phylogenetic placement of the crocodile skinks (Tribolonotus): Bayesian approaches to assessing congruence and obtaining confidence in maximum likelihood inferred relationships. Mol. Phylogenet. Evol. 27:384–397.

Revell LJ. 2009. Size correction and principal components for interspecific comparative studies. Evolution 63:3258–3268.

Revell L.J., Mahler D.L., Peres-Neto P.R., Redelings B.D. 2012. A new method for identifying exceptional phenotypic diversification. Evolution 66:135–146.

Reznick D.N., Ricklefs R.E. 2009. Darwin's bridge between microevolution and macroevolution. Nature 457:837–842.

Rosenzweig M.L. 1995. Species diversity in space and time. Cambridge: Cambridge University Press.

Schluter D. 2000. Ecology of adaptive radiation. Oxford: Oxford University Press.

Sepkoski J.J. 1978. A kinetic model of Phanerozoic taxonomic diversity I. Analysis of marine orders. Paleobiology 4:223–251.

Skinner A. 2007. Phylogenetic relationships and rate of early diversification of Australian *Sphenomorphus* group scincids (Scincoidea, Squamata). Biol. J. Linn. Soc. 92:347–366.

Skinner A. 2010. Rate heterogeneity, ancestral character state reconstruction, and the evolution of limb morphology in *Lerista* (Scincidae, Squamata). Syst. Biol. 59:723–740.

Skinner A., Hugall A.F., Hutchinson M.N. 2011. Lygosomine phylogeny and the origins of Australian scincid lizards. J. Biogeog. 38:1044–1058.

Skinner A., Hutchinson M.N., Lee M.S.Y. 2013. Phylogeny and divergence times of Australian *Sphenomorphus* group skinks (Scincidae, Squamata). Mol. Phyl. Evol. 69:906–918.

Skinner A., Lee M.S.Y, Hutchinson M.N. 2008. Rapid and repeated limb loss in a clade of scincid lizards. BMC Evol. Biol. 8:310.

Thomas G.H., Freckleton R.P. 2012. MOTMOT: models of trait macroevolution on trees. Methods Ecol. Evol. 3:145–151.

Venditti C., Meade A., Pagel M. 2011. Multiple routes to mammalian diversity. Nature 479:393–396.

Vermeij G.J. 1973. Adaptation, versatility, and evolution. Syst. Zool. 22:466–477.

Weir J.T., Mursleen S. 2013. Diversity-dependent cladogenesis and trait evolution in the adaptive radiation of the auks (Aves: Alcidae). Evolution 67:403–416.

Yang Z., Rannala B. 1997. Bayesian phylogenetic inference using DNA sequences: a Markov chain Monte Carlo method. Mol. Biol. Evol. 14:717–724.

Yoder J.B., Clancey E., Des Roches S., Eastman J.M., Gentry L., Godsoe W., Hagey T.J., Jochimsen D., Oswald B.P., Robertson J., Sarver B.A., Schenk J.J., Spear S.F., Harmon L.J. 2010. Ecological opportunity and the origin of adaptive radiations. J. Evol. Biol. 23:1581–1596.